"Synapsable" DNA Double Helices: Self-Selective Modules for Assembling DNA Superstructures

Richard P. Fahlman and Dipankar Sen*

Contribution from the Institute of Molecular Biology & Biochemistry and Department of Chemistry, Simon Fraser University, Burnaby, British Columbia V5A 1S6, Canada

Received July 20, 1999

Abstract: Much recent interest has focused on DNA as a material for the construction of two- and three-dimensional objects on the nanometer to micrometer scale. Such constructions have made use of the recognition of "complementary" nucleotide sequence by single-stranded stretches of DNA and the formation of double helices (duplexes) via the formation of Watson−Crick base pairs. Recently, we have described a quite distinct paradigm for the side-by-side binding ("synapsis") by two intact DNA duplexes modified by the inclusion of short elements of eight guanine-guanine mismatch base pairs (a "G-G domain") within them. Here, we demonstrate that it is possible to design nonidentical G-G domains, which have the property of synapsing exclusively to "self" as opposed to "non-self". Two modes of synapsis are observed in this versatile system: that in which two distinct species of duplex in a mixture concertedly undergo "self"-synapsis and that in which one designated species out of the two "self"-synapses specifically. Incorporation of these novel methodologies for "self"-synapsis and site-specific synapsis by DNA duplexes into current methods for constructing DNA nanostructures and mesostructures may facilitate the assembly of more complex DNA-based materials and arrays.

Introduction

Recently, much interest has focused on the use of DNA for the construction of molecular superstructures on the nanometer to micrometer scale. DNA has been utilized for the construction of various three-dimensional objects of defined topology;[1] in addition, the property of sequence complementarity recognition by individual DNA single strands has been used to assist the assembly of other materials, such as gold microbeads, into near-crystalline arrays.[2−5] Two fundamental properties of DNA make it especially suitable as a raw material for such constructions: (a) the above-mentioned highly specific recognition of sequence complementarity by individual DNA strands, and the assembly on that basis of two complementary strands into double helices, and (b) the fact that, in aqueous solutions, a DNA double helix has the physical and hydrodynamic properties of a rigid rod, with a persistence length of 28−35 nm (80−100 base pairs) in 1 M sodium chloride (and substantially longer persistence lengths at lower salt).[6] The above properties make DNA a potentially interesting "material".

The use of DNA in the construction of geometric objects has been pioneered by Seeman, who has described objects with the topologies of, for instance, a tetrahedron[7] and a truncated octahedron.[8] The modules for such constructions were stable three-way and four-way immobile junctions of DNA duplexes
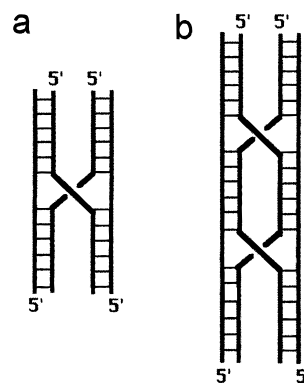

Figure 1. Schematics for (a) a stable four-way junction of DNA duplexes and (b) a double-crossover.

(Figure 1a shows a schematic for a four-way junction). Each double-helical arm of such a junction terminated in a short stretch of single-stranded DNA of defined sequence (a "sticky end"), which was used to bind, on the basis of precise sequence complementarity, to the sticky ends of other three- or four-way junctions. More recently, Seeman has utilized a more rigid structural unit, the DNA "double-crossover", composed of two closely spaced four-way junctions (Figure 1b), to assemble two-dimensional quasi-crystalline arrays,[9−11] as well as to construct a mechanical device that exploits the conversion of a stretch of right-handed B-DNA duplex into a left-handed Z-DNA duplex.[12]

* Corresponding author.

(1) Seeman, N. C. *Annu. Rev. Biophys. Biomol. Struct.* **1998,** *27,* 225−248.

(2) Mirkin, C. A.; Letsinger, R. L.; Mucic, R. C.; Storhoff, J. J. *Nature* **1996,** *382,* 607−609.

(3) Alivisatos, A. P.; Johnsson, K. P.; Peng, X.; Wilson, T. E.; Loweth, C. J.; Bruchez, M. P., Jr.; Schultz, P. G. *Nature* **1996,** *382,* 609−611.

(4) Mucic, R. C.; Storhoff, J. J.; Mirkin, C. A.; Letsinger, R. L. *J. Am. Chem. Soc.* **1998,** *120,* 12674−12675.

(5) Loweth, C. J.; Caldwell, W. B.; Peng, X.; Alivisatos, A. P.; Schultz, P. G. *Angew. Chem., Int. Ed.* **1999,** *38,* 1808−1812.

(6) Hagerman, P. J. *Annu. Rev. Biophys. Biophys. Chem.* **1988,** *17,* 265−286.

(7) Chen, J.; Seeman, N. C. *Nature* **1991,** *350,* 631−633.

(8) Zhang, Y.; Seeman, N. C. *J. Am. Chem. Soc.* **1994,** *116,* 1661−1669.

(9) Winfree, E.; Liu, F.; Wenzler, L. A.; Seeman, N. C. *Nature* **1998,** *394,* 539−544.

(10) Liu, F.; Sha, R.; Seeman, N. C. *J. Am. Chem. Soc.* **1999,** *121,* 917−922.

(11) Mao, C.; Sun, W.; Seeman, N. C. *J. Am. Chem. Soc.* **1999,** *121,* 5437−5443.

(12) Mao, C.; Sun, W.; Shen, Z.; Seeman, N. C. *Nature* **1999,** *397,* 144−146.
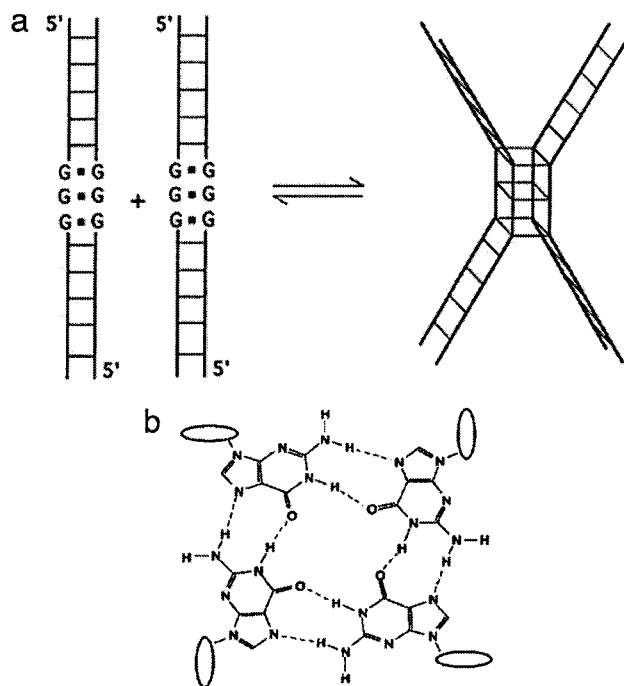
Figure 2. Schematics for (a) two synapsable DNA duplexes, each containing a G-G domain, undergoing synapsis to form a synapsed duplex dimer, and (b) a guanine quartet (G-quartet). Each guanine base is attached via its 9-position to a deoxyribose sugar (indicated by an ovoid shape).

We have recently described a quite different paradigm for the stable self-association of two DNA double helices, one that does not exploit sticky end complementarity. This methodology involves a side-by-side association, or "synapsis", of two DNA duplexes, at predetermined "synapsable" sites constructed within them (Figure 2a). Unlike single-stranded DNA, standard DNA duplexes have little ability to interact with one another. This is due to the facts that two duplexes do not have significant shape complementarity; that the DNA bases, with their hydrogen-bonding and π-stacking ability, are fully base-paired in a Watson−Crick sense (A=T; G≡C) in the interior of the double helix; and that the sugar−phosphate backbones of duplexes possess high (and therefore mutually repulsive) negative charge densities. However, the simple innovation of introducing a stretch of contiguous guanine-guanine mismatch base pairs (called a "G-G domain") into an otherwise standard Watson−Crick base-paired duplex (shown schematically in Figure 2a) has been shown to enable a stable side-to-side association and binding of two such duplexes under physiological and near-physiological conditions of temperature and salt.[13] A DNA duplex incorporating a G-G domain is referred to as a "synapsable" DNA duplex. Two such duplexes are able to dimerize via synapsis of their respective G-G domains to form "duplex dimers", held together by a very stable hydrogen-bonded arrangement of guanine bases known as a guanine quartet (Figure 2b).[14,15] In other contexts, the formation of guanine quartets and guanine quadruplexes (DNA structures composed of, or containing, guanine quartets) in aqueous solutions has been shown to be favored by the presence of specific Group IA and IIA cations, notably potassium and strontium (and, less effectively, by sodium and rubidium; calcium and barium), which bind within the cavity formed between two adjacent

guanine quartets.[14,15] The dimerization of synapsable duplexes was also found to follow this general trend.[13,16] Given that different Group IA and IIA cations differentially stabilized the duplex dimers (for instance, potassium was strongly stabilizing, whereas lithium was not), the assembly and disassembly of superstructures built with duplex dimer modules might, in principle, be achievable by simply changing the cation present in solution−for instance, replacing 0.5 M Li$^+$ for 0.5 M K$^+$, and vice versa.

Earlier studies on synapsable DNA duplexes[13,16] had focused on the dimerization properties of duplexes that were 48−52 base pairs long and contained G-G domains composed of eight contiguous G-G mismatch base pairs. A major question that remained was whether it might be possible to design a variety of different G-G domains, such that each one was specific for "self"-synapsis. For instance, in the simplest case, whether from a mixed solution of duplexes containing synapsable domains "*a*" and "*b*", only the a_2 and b_2, and not the *a.b* types of synapsed duplex dimers might be obtained. In this paper, we demonstrate that it is, indeed, possible to design such non-equivalent synapsable G-G domains, which have the property of "self"-synapsis. We demonstrate further that, from a solution containing a mixture of *a* and *b*, it is possible, utilizing small variations in the incubation conditions, to generate the a_2 and b_2 complexes simultaneously, a_2 alone, and b_2 alone. In none of the above incubations is the *a.b* product observed.

Materials and Methods

DNA Synthesis and Purification. The two DNA oligomers used to construct the J·K duplex had the following sequences (the underlined sequences indicate the bases designated to form its G-G domain in the assembled duplex):

J = 5′-GTGAC TCGAG AAGCT CCTGA
         TTGGT TGGGG GTTTG TGGTT CAAGG ATCCA CAG

K = 5′-CTGTG GATCC TTGAA CCACA
         TTGGG GGTTG GTTTC AGGAG CTTCT CGAGT CAC

The oligomers for the L·M duplex were as follows:

L = 5′-CTCGA GAAGC TCCTG ATTGG GTGGG TTTGT
                                    GGTTC AAGGA TCC

M = 5′-GGATC CTTGA ACCAC ATTGG GTGGG TTTCA
                                    GGAGC TTCTC GAG

The oligomers for the H·I duplex were as follows:

H = 5′-TGACT CGAGA AGCTC CTGAT TGGGG GTTTG
                                    TGGTT CAAGG ATCCA CA

I = 5′-TGTGG ATCCT TGAAC CACAT TGGGG GTTTC
                                    AGGAG CTTCT CGAGT CA

The oligomers for the three-way junction were as follows:

W(H·I)T(L·M) = 5′-TGCAG TTGAG TTGGG TGGGT TCTGG
CGAAC GGACG TTGCA GGCTT TTGCC TGCCA CCGGC
                   GGAAG CTCTT GGGGG TTGCG ACGAT GG

C(H·I)T(L·M) = 5′-CCATC GTCGC TTGGG GGTTG
    AGCTT CCGCC GGTGC GTCCG TTCGC
                   CAGTT GGGTG GGTTC TCAAC TGCA

(13) Venczel, E. A.; Sen, D. *J. Mol. Biol.* **1996**, *257*, 219−224.
(14) Williamson, J. R. *Annu. Rev. Biophys. Biomol. Struct.* **1994**, *23*, 703−730.
(15) Wellinger, R.; Sen, D. *Eur. J. Cancer* **1997**, *33*, 735−749.

(16) Fahlman, R. P.; Sen, D. *J. Mol. Biol.* **1998**, *280*, 237−244.

"Synapsable" DNA Double Helices

J. Am. Chem. Soc., Vol. 121, No. 48, 1999 11081

All oligomers were synthesized at the University of Calgary Core DNA Services. Crude oligomer samples were dissolved in 50 μL of denaturing gel-loading buffer (0.25% bromophenol blue; 0.5% xylene cyanol FF, 30% glycerol; 10 mM Tris-Cl, pH 7.5), heated at 95 °C for 3 min to break down any preformed G-quadraplex complexes, and size-fractionated in 8% (w/v) denaturing polyacrylamide gels. The DNA bands in the gel were visualized by UV-shadowing and excised, and the DNA was recovered by overnight elution into TE buffer (10 mM Tris, pH 7.9; 0.1 mM EDTA). The DNA solutions were filtered through 0.2-μm microfilters (Gelman Sciences) and desalted and concentrated using C-18 Spice Columns (Analtech). The lyophilized pellets of purified DNA were finally dissolved in 50 μL of TE buffer. 5′ end-labeling with [γ-^{32}P]ATP was carried out using standard kinasing protocols.[17] Ethanol precipitations of the DNA, where necessary, were carried out by adding 2.5 vol of EtOH to aqueous DNA solutions made up to 0.8 M LiCl.

Preparation of Double-Stranded DNA. All duplexes and the three-way junction were assembled by mixing in water at room temperature 500 pmol of a given oligomer with 500 pmol (470 pmol of unlabeled and 30 pmol of 5′-^{32}P-labeled) of its complementary oligomer. The oligomer mixtures were made up to TMACl buffer [100 mM tetra-methylammonium chloride (TMACl); 10 mM Tris, pH 7.9], heated to 95 °C for 2 min, and allowed to cool slowly to 30 °C. The resulting duplex DNA samples were purified by loading in 8% nondenaturing polyacrylamide gels, which were electrophoresed in TBT buffer (50 mM Tris−borate, pH 8.0; 10 mM TMACl) at 6 W at room temperature. Bands of duplex DNA in the gel were detected by autoradiography and excised, and the DNA was eluted into 2× TMACl buffer. Eluted samples were concentrated using Microcon microconcentrators (Amicon) with a 10-kD molecular weight cutoff.

Formation of Synapsed Duplex Dimers and Three-Way Junction Dimers. Duplex DNA samples, as prepared above, were diluted with 2× TMACl buffer to 2 times the final DNA concentration to be used for dimerizations. Samples containing more than one duplex were also prepared in this fashion. Aliquots of 5 μL of such duplex DNA solutions were combined with 5 μL of various salt solutions and incubated at 37 °C for different times. Tightly sealed 100-μL tubes were used throughout, and the tubes were completely immersed in a water bath at 37 °C to prevent changes in the sample volume from evaporation and condensation. For analysis, aliquots were removed from each sample, combined with nondenaturing gel-loading buffer, and run in 8% nondenaturing polyacrylamide gels (6% gels were used for the three-way junction sequences) run in KMg buffer (50 mM Tris−borate, pH 8.0; 10 mM KCl; 2 mM MgCl$_2$) at 6 W at 4 °C, unless stated otherwise. Gels were then dried and radioactive bands visualized and assayed using a BioRad GS-250 molecular imager.

Melting Point Determinations. Melting points of duplex DNA samples were determined spectrophotometrically using a Cary 300 Bio UV−visible spectrophotometer with a temperature controller (Varian). The absorbance at 260 nm of 0.3 μM samples of duplex DNA were monitored from 37 to 90 °C, with a heating rate of 0.1 °C/min. Absorbance profiles were analyzed with the Cary Thermal Software v1.00(6).

The melting behavior of synapsed duplex dimers was followed most accurately by electrophoretic methods. Samples were prepared as described above, with prolonged incubations to ensure that equilibrium had been reached in the formation of synapsed duplex dimers. Samples were then diluted to 0.1 μM total DNA, while the salt concentration (1 M KCl in TMACl buffer) was kept constant. The diluted samples were incubated at 37 °C for 1 h and then subjected to a routine where they were heated for 15 min each at a series of progressively increasing temperatures, from 50 to 95 °C, in 5 °C steps. Following each incubation at a given temperature, 2-μL aliquots were removed and mixed into 3 μL of nondenaturing gel-loading buffer solution on ice. After being left on ice for 3 min, each sample was loaded into an 8% nondenaturing gel run in KMg buffer (see above) for analysis.

Methylation Protection Assays. Methylation experiments were carried out using a modified version of the DNA sequencing procedure

(17) Sambrook, J.; Fritch, E.; Maniatis, T. *Molecular Cloning. A Laboratory Manual,* 2nd ed.; Cold Spring Harbor Laboratory Press: Cold Spring Harbor, NY, 1989; Vol 2.

Figure 3. G-G domains of synapsable duplexes J·K and L·M. The highlighted bases constitute the G-G domains, and boxes surround G-G mismatch base pairs.

of Maxam and Gilbert.[18] DNA samples (10 μL; 5 μM final) were incubated in solutions containing 1 M LiCl in TMACl buffer (where synapsis was not desired), or in 1 M KCl in TMACl buffer (where synapsis was desired). Following overnight incubations at 37 °C, each sample was combined with 3.3 μL of 200 mM lithium cacodylate (pH 7.5) and made up to 0.1−0.4% (v/v) dimethyl sulfate (DMS). Methylation was allowed to proceed at 37 °C for 30 min, and each sample was then combined with 5 μL of nondenaturing loading buffer and run in 8% nondenaturing gels run in KMg buffer (see above). The wet gels were exposed to X-ray film, and bands corresponding to DNA duplexes and synapsed duplex dimers were cut out of the gel. The DNA from all excised gel bands was eluted into 300 μL of TE buffer overnight and recovered by ethanol precipitation (see above). The purified and washed DNA pellets were dissolved in 50 μL of 10% (v/v) piperidine in water and heated at 90 °C in sealed tubes for 30 min. Following this treatment, the samples were lyophilized to remove water and piperidine, and the DNA was dissolved in denaturing gel-loading buffer. Samples containing equal counts of radioactivity were loaded and run in 10% sequencing gels run at 25 W. The gels were dried, and the radioactive DNA bands were visualized using a BioRad GS-250 molecular imager.

Results and Discussion

Design of Self-Selective Synapsable DNA Duplexes. Prior studies on synapsable DNA duplexes had utilized duplexes that contained stretches of eight contiguous G-G mismatches within their synapsable G-G domains.[13] These experiments left open the question of whether more than one kind of G-G domain, e.g., *a*, *b*, and *c*, could be used for synapsis, such that domain *a* was specific for synapsing only with another *a*, and not with *b* or *c*. We therefore designed two divergent G-G domains by interspersing T-T base mismatches among the G-G mismatches to spatially separate contiguous G-G domains. T-T mismatches were chosen in part because prior work[13,16] had indicated that their presence at the ends of G-G domains did not interfere with the latters' synaptic properties. Two different synapsable duplexes, J·K and L·M, were thus created (Figure 3). We postulated that *self-* or *homo-*synapsis by each of these duplexes would potentially form a larger number of guanine quartets [upto seven in (J·K)$_2$ and six in (L·M)$_2$] than might form from *cross-* or *hetero-*dimerization of the duplexes [at best, five quartets in the hetero-synapse (J·K)·(L·M)]. We therefore surmised that, at equilibrium, the greater predicted thermodynamic stability of the two homo-synapsed dimers might lead to their accumulation relative to the hetero-synapsed dimer.

Synaptic Dimerization of J·K and L·M Duplexes. The individual abilities of the duplexes J·K and L·M to dimerize via synapsis was examined in the presence of 1 M concentrations of different alkali cations at 37 °C. Conventionally, G-quadruplex formation (whether starting with single-stranded DNA or with synapsable duplexes) follows the ion preference of K$^+$ > Rb$^+$, Na$^+$ ≫ Li$^+$, Cs$^+$.[14,15] Figure 4 shows that L·M

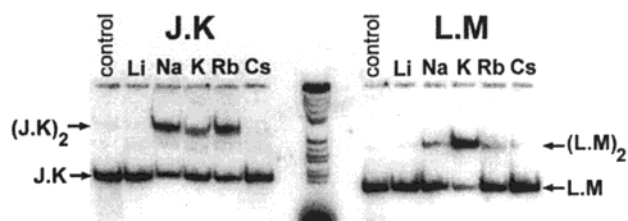(18) Maxam, A. M.; Gilbert, W. *Proc. Natl. Acad. Sci. U.S.A.* **1977**, *74*, 560−564.

Figure 4. Nondenaturing polyacrylamide gels showing the influence of the different alkali cations on the synaptic dimerization of the J·K and L·M duplexes. Samples of 2.0 μM duplex DNA (J·K and L·M) were incubated at 37 °C for 48 h in the presence of different alkali chlorides. Control samples contained 100 mM TMACl and 10 mM Tris (pH 7.9), while the other samples were incubated in 1 M XCl (where X = Li, Na, K, Rb or Cs), 100 mM TMACl, and 10 mM Tris (pH 7.9).
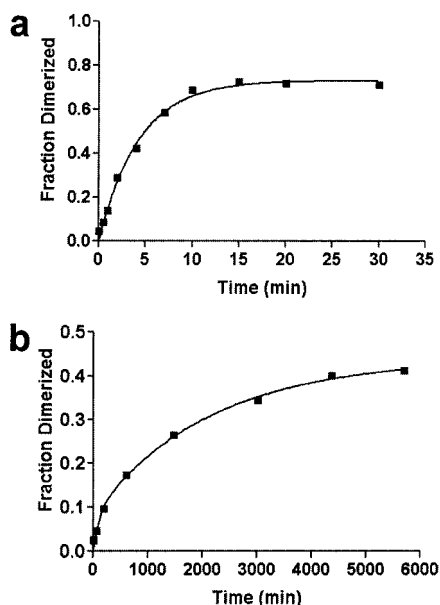

Figure 5. Time dependences for the synaptic dimerization of L·M (a) and J·K (b) into their respective duplex dimers. The duplex concentrations used were 0.5 μM for L·M and 2.5 μM for J·K. Samples were incubated in 1 M KCl, 100 mM TMACl, 10 mM Tris (pH 7.9) at 37 °C.

exhibited the above cation preference for its dimerization. However, an anomalous cation preference was observed for the dimerization of the J·K duplex, with both Na^+ and Rb^+ supporting a larger yield of dimerized product than K^+ (Figure 4). Such anomalous cation preferences for the formation of certain specific G-quadruplex structures have been reported[16,19] and are generally the consequence of the formation and stabilization by the highly stabilizing potassium ion of alternative G-quadruplex complexes. A mechanistic model for the observed anomalous ion dependence for the formation of (J·K)$_2$ is given below.

In addition to the divergent alkali cation dependences for the formation of (J·K)$_2$ and (L·M)$_2$, the rates of formation of these two complexes were found to be remarkably different. Figure 5 shows that the synaptic dimerization of 0.5 μM L·M reached equilibrium almost 1000 times faster than that of 2.5 μM J·K when both were measured under standardized dimerization conditions (1 M KCl in TMACl buffer at 37 °C). The dimerization of duplex L·M followed second-order kinetics, with an observed rate constant of $(1.5 \pm 0.3) \times 10^5$ M^{-1} min^{-1} under the above standard conditions. Using the K_d value of 130 ± 70 nM computed from the equilibrium distribution of L·M and (L·

(19) Sen, D.; Gilbert, W. *Nature* **1990**, *344*, 410−414.

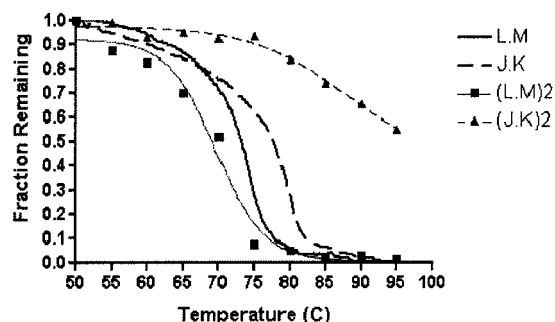**Figure 6.** Thermal melting profiles of the duplexes J·K and L·M and of their duplex dimers.

M)$_2$ under these conditions, a dissociation rate constant for (L·M)$_2$ to L·M of 0.025 ± 0.014 min^{-1} was calculated. A comparison of the rate of L·M dimerization with that of the formation of duplexes from single-stranded DNA (2.6 × 10^8 M^{-1} min^{-1} at 32.5 °C and 1.14 × 10^8 M^{-1} min^{-1} at 40.2 °C)[20] indicated that the L·M duplex dimerized less than a 1000-fold slower than duplex formation by single-stranded DNA. In contrast, other G-quartet-forming sequences exhibit significantly slower kinetics of formation than the dimerization of L·M, with typical rates of between 6 and 300 M^{-1} min^{-1}.[21−23]

The dimerization of the J·K duplex did not follow simple second-order kinetics. The formation curve for (J·K)$_2$ formation (Figure 5b) showed at least two components. We postulated that this complexity of kinetics was related to this duplex's unusual ion preference for dimerization (Figure 4). A possibility was that the J·K duplex, in the presence of potassium, existed in two interchanging conformational forms, J·K and J·K′, of which J·K′ perhaps was incapable of synaptic dimerization (owing possibly to the presence of *intra*molecular G-quartets within its own structure). Experiments to determine the existence and nature of such a putative J·K′ conformer are described below.

Duplex Dimer Stability. The thermal stabilities of the synapsable duplexes J·K and L·M duplexes were measured in 1 M LiCl in TMACl buffer, using standard UV spectrophotometric techniques. Figure 6 shows the absorbance data for the two duplexes as functions of temperature. The melting points of the duplexes were determined to be 80.4 and 74.4 °C, respectively, and the melting behavior of both duplexes was cooperative, as is found for standard DNA duplexes.

The melting behavior of the duplex dimers (J·K)$_2$ and (L·M)$_2$ was most conveniently measured using gel electrophoretic techniques.[13,16] Owing to the high double-stranded DNA content (relative to quadruplex content) of both (J·K)$_2$ and (L·M)$_2$, the dimer dissociation is difficult to monitor spectroscopically, owing to the large spectroscopic contribution of those double-stranded arms. Preformed duplex dimer samples were diluted to lower their DNA concentration to <100 nM, such that a reassociation of dissociated duplex dimers was essentially undetectable within the experimental time scale. The samples' ionic strength was maintained at 1 M KCl in TMACl buffer. The melting behaviors of (J·K)$_2$ and (L·M)$_2$ were then measured as described in Materials and Methods. Figure 6 shows that the (L·M)$_2$-to-L·M transition was cooperative and had a midpoint of ∼71 ± 2 °C. The (J·K)$_2$ complex was, by contrast, more

(20) Pörschke, D.; Eigen, M. *J. Mol. Biol.* **1971**, *62*, 361−381.
(21) Guo, Q.; Lu, M.; Markey, L. A.; Kallenbach, N. R. *Biochemistry* **1992**, *31*, 2451−2455.
(22) Guo, Q.; Lu, M.; Kallenbach, N. R. *J. Biol. Chem.* **1992**, *267*, 15293−15300.
(23) Fang, G.; Cech, T. R. *Biochemistry* **1993**, *32*, 11646−11657.
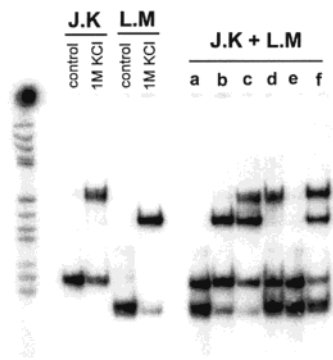
Figure 7. Self-selectivity of J·K and L·M dimerization. Samples of J·K and L·M alone (left panel) contain 2.0 μM dsDNA in TMACl buffer (100 mM TMACl) and 10 mM Tris (pH 7.9), with and without 1 M KCl. These samples were incubated at 37 °C for 72 h. Mixed samples containing 2.0 μM each of the J·K and L·M duplexes are shown in lanes a−f, in all cases incubated in TMACl buffer with or without additional salts, at 37 °C and for 72 h, unless otherwise stated. Lane a, control mixture of J·K and L·M in TMACl buffer. Lanes b and c, incubations in TMACl buffer containing 1 M KCl; lane b shows a 20-min incubation, lane c shows a 72-h incubation. Lane d, the effect of diluting a preincubated sample (as in lane c) to a KCl concentration of 10 mM. Lane e, incubation in 10 mM KCl. Lane f, incubation in 1 M NaCl.

stable and did not describe a complete melting curve by 95 °C. In fact, the broad initial phase (from 75 to 95 °C) of $(J \cdot K)_2$ breakdown may represent the breakdown of a proportion of $(J \cdot K)_2$ complexes containing fewer G-quartets than the bulk of the $(J \cdot K)_2$ complexes (from a "slipped" or imperfectly aligned side-by-side arrangement of the two participating J·K duplexes). Alternatively, this initial phase of $(J \cdot K)_2$ breakdown may reflect very slow kinetics of dissociation (on the experimental time scale) of the $(J \cdot K)_2$ complex. In either event, it was clear that the $(J \cdot K)_2$ dimer was significantly more stable than the $(L \cdot M)_2$ dimer.

Self-Selectivity of Synaptic Dimerizations. To determine whether the duplexes would cross-react to form *hetero*-dimers, solutions containing both duplexes, J·K and L·M, were incubated under standard dimerization conditions (see above). Figure 7 shows these results. It had been shown previously that if two synapsable duplexes, e.g., W·X and Y·Z, containing the *same* synapsable G-G domain, but being of different overall lengths (and therefore having different electrophoretic mobilities), were allowed to dimerize together, a hetero-dimer $(W \cdot X) \cdot (Y \cdot Z)$ formed, in addition to the $(W \cdot X)_2$ and $(Y \cdot Z)_2$ homo-dimers. Being of intermediate molecular weight, the $(W \cdot X) \cdot (Y \cdot Z)$ complex ran in the gel between the $(W \cdot X)_2$ and $(Y \cdot Z)_2$ complexes; in other words, a total of three product bands was seen.[13] Figure 7, lane C, shows that, when a dimerization mixture containing J·K and L·M was allowed to reach equilibrium in 1 M KCl at 37 °C, only the two bands corresponding to the homo-dimer products $(J \cdot K)_2$ and $(L \cdot M)_2$ were observed. Therefore, dimerization by these two duplexes appeared to be *self-specific*.

Furthermore, if the same dimerization mixture was incubated briefly (~20 min), such that equilibrium was not reached, only the $(L \cdot M)_2$ product was observed (Figure 7, lane B). Therefore, the rapid kinetics of $(L \cdot M)_2$ formation could be exploited to obtain just this dimer out of a J·K and L·M mixture. Analogously, we found that the greater thermodynamic stability of $(J \cdot K)_2$ could be taken advantage of to obtain only the $(J \cdot K)_2$ complex out of the same dimerization mixture. If the 1 M ionic strength of a solution containing an equilibrium distribution of J·K, L·M, $(J \cdot K)_2$, and $(L \cdot M)_2$ was diluted to a final salt
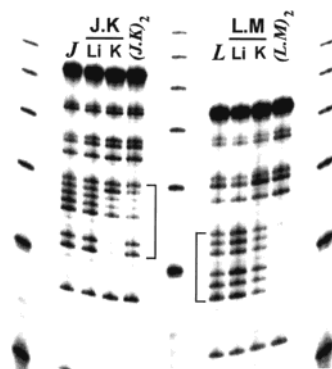

Figure 8. Sequencing gels showing methylation protection of guanine bases. DNA samples were partially methylated by DMS and cleaved at methylated sites with piperidine as described in the Materials and Methods section. All methylation reactions were carried out in TMACl buffer at 37 °C. Lanes J and L display the patterns of the single-stranded DNA sequences J and L methylated in 1 M LiCl. Lanes containing the duplex DNA samples, J·K and L·M, were methylated either in 1 M LiCl or in 1 M KCl (as indicated). Methylation of the duplex dimers, lanes $(J \cdot K)_2$ and $(L \cdot M)_2$, was carried out in 1 M KCl.

concentration of 10 mM KCl in TMACl buffer, and the diluted solution was incubated at 37 °C for 20 min, $(L \cdot M)_2$ was found to selectively dissociate (Figure 7, lane D). Lane E shows that, under these low salt conditions for the selective breakdown of $(L \cdot M)_2$, neither J·K nor L·M was able to dimerize, even after 3 days of incubation.

The above experiments demonstrated the high versatility of this system, such that, from a single starting solution containing the J·K and L·M duplexes, we were able to obtain at will a $(J \cdot K)_2$ synapsis, a $(L \cdot M)_2$ synapsis, or both synapses at the same time. Control incubations with single-stranded J and L oligomers carried out in 1 M KCl at 37 °C indicated that these oligomers formed J_4 and L_4 quadruplexes, as expected, but also cross-associated to give the series of complexes J_3L, J_2L_2, etc. (data not shown). Therefore, the specificity of self-association described above was unique to the J·K and L·M *duplexes* and not to their component single strands. This example of self-selectivity by G-quadruplex-forming DNA species is currently unique.

Duplex J·K Forms a Dimerization-Incompetent Conformer, J·K′. To understand the molecular events that permitted self-selective synaptic dimerizations by J·K and L·M to occur out of mixtures of the two duplexes, it was necessary to examine both the anomalous kinetics and the cation preference observed for the formation of $(J \cdot K)_2$. To do this, we examined precisely which of the guanines in J·K were, under different solution conditions, involved in G-quartet formation, to determine whether *intra*-molecular G-quartets could form in the undimerized J·K duplex. The technique used for this investigation was methylation protection. Guanines that are involved in G-quartet formation (unlike those that either are not base-paired or are involved in Watson−Crick G≡C base pairs) are resistant to methylation by dimethyl sulfate (DMS) at their N-7 positions, and this "protection" from methylation can be used to pinpoint those guanines in a synapsable duplex or in a synapsed duplex dimer that are participating in a guanine-quartet.[24]

The results of the DMS probing of J, L, J·K, L·M, $(J \cdot K)_2$, and $(L \cdot M)_2$ are shown in Figure 8 as sequencing gels, with the guanines in strands J and L, respectively, being examined in all cases. As expected, in the duplex dimers $(J \cdot K)_2$ and $(L \cdot M)_2$, the guanines in the respective G-G domains (indicated within

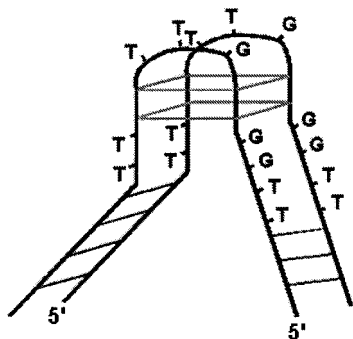(24) Sen, D.; Gilbert, W. *Nature* **1988**, *334*, 364−366.

Figure 9. Model for the potassium conformer of J·K, the J·K′ "pinched" duplex.

brackets) showed methylation protection of all or some of the guanines within the domains, relative to the duplex samples methylated in LiCl. The $(L·M)_2$ duplex dimer exhibited complete protection of its mismatch guanines, while $(J·K)_2$ exhibited only a partial protection—of five of its seven mismatch guanines. It was the J·K and the L·M samples in potassium solutions that showed the most revealing results. Whereas the L·M duplex showed similar methylation patterns of its G-G domain guanines in both lithium and potassium solutions [the slight protection of all the domain guanines in potassium was probably due to a partial interconversion of L·M and $(L·M)_2$ within the methylation time scale], the J·K duplex in potassium solution showed a quite different protection pattern from its counterpart in lithium solution. In the J·K sample in potassium, the two isolated guanines of its motif TT<u>GG</u>TTGGGGGTT were fully methylation-protected, along with two of the guanines out of the remaining stretch of five. This protection pattern was highly suggestive of the possibility that, even in its duplex form, J·K formed a significant conformer, J·K′, which already contained G-quartets, thus rendering this conformer incapable of dimerizing to $(J·K)_2$. A schematic diagram for the structure of the conformer J·K′, which we term a "pinched" duplex, is given in Figure 9.

To test our hypothesis that the above model was true, a simplified version of the J·K G-G domain was created. The new duplex, H·I, had the domain sequence of TTGGGGGTT, which would be expected to lack the ability to fold back to form intramolecular G-quartets, such as those found within J·K. As predicted, the H·I duplex exhibited a normal preference for the alkali cations: $K^+ > Na^+ \approx Rb^+ > Li^+ \approx Cs^+$, unlike J·K but similar to L·M (data not shown). Duplex H·I also dimerized significantly faster than J·K and exhibited second-order kinetics with a rate constant of $(3.3 \pm 0.8) \times 10^3$ $M^{-1}min^{-1}$ at 37 °C in 1 M KCl. The dissociation constant for the $(H·I)_2$ dimer was determined to be 76 ± 40 nM under the same conditions. Methylation studies of the H·I duplex also showed, predictably, that the reactivity patterns of domain guanines in H·I were equivalent in lithium and potassium solutions (data not shown).

To test whether the self-selectivity of synapsis that we had observed from mixtures of J·K and L·M was observable also from mixtures of H·I and L·M, incubations for dimerization in 1 M KCl were carried out. As with the J·K and L·M combination, no hetero-dimer product $(H·I)·(L·M)$ was observed, even when incubations were carried out at the permissive temperature of 4 °C in 1 M KCl.

A "Tile" for the Assembly of DNA Superstructures. We constructed a three-way junction of DNA duplexes, $(H·I)T(L·M)$, two of whose arms contained, respectively, the G-G domains of H·I and L·M ("h·i" and "l·m", Figure 10A). The
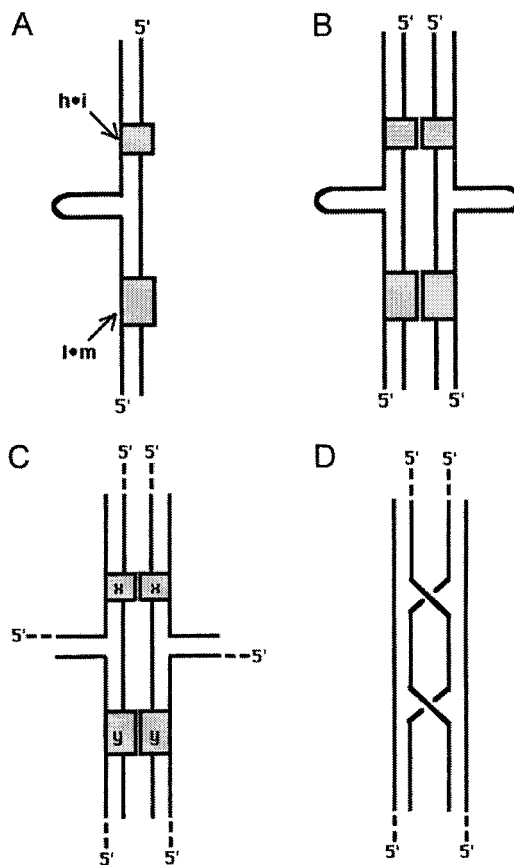

Figure 10. Schematics of (A) the three-way junction (H·I)T(L·M); (B) the synapsed duplex dimer $[(H·I)T(L·M)]_2$; (C) a $[(H·I)T(L·M)]_2$-like "tile", with six sticky ends (shown by dashed lines); and (D) a double-crossover, with four sticky ends.

junction itself had been studied by high-resolution NMR by Leontis et al.,[25] who found that it preferred to adopt a "T"-like conformation of the three arms (rather than a "Y"-like conformation). $(H·I)T(L·M)$ was simply constructed by annealing together two synthetic single-stranded DNA oligomers (see Materials and Methods). On incubation of $(H·I)T(L·M)$ with potassium, a predominant higher-order complex formed rapidly and almost quantitatively (Figure 11). Evidence that this was the dimeric product $[(H·I)T(L·M)]_2$ (shown schematically in Figure 10B) was obtained from methylation protection experiments (data not shown), which revealed that both the h·i and l·m domains showed the methylation protection patterns characteristic of their having undergone synapsis. When methylation protection experiments were carried out in a time-dependent manner, it was found that, as expected, that the l·m domain synapsed first, in the first 10 min, followed by the h·i domain. That $[(H·I)T(L·M)]_2$ was held together at both the h·i and l·m synaptic sites was suggested further by the fact that this complex was fully stable to melting even at 95 °C, at which temperature the individual $(H·I)_2$ (which melted at 88 ± 2 °C, data not shown) and $(L·M)_2$ duplex dimers had either melted or begun to melt (see Figure 6). The use of the G-G domains h·i as well as l·m to generate the $[(H·I)T(L·M)]_2$ complex (rather than with two copies of either h·i or l·m) was necessary to ensure that a defined spatial and orientational relationship of the various double-helical arms of the $[(H·I)T(L·M)]_2$ product was obtained.

The $[(H·I)T(L·M)]_2$ complex may be regarded as a structural "tile" for the assembly of DNA superstructures, and, as shown

(25) Leontis, N. B.; Hils, M. T.; Piotto, M.; Malhotra, A.; Nussbaum, J.; Gorenstein, D. G. *J. Biomol. Struct. Dyn.* **1993**, *11*, 215−223.
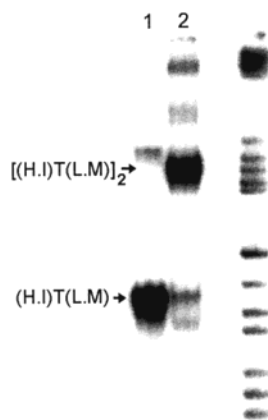
Figure 11. Dimerization of the (H·I)T(L·M) three-way junction. Samples containing 1.0 μM (H·I)T(L·M) were incubated in TMACl buffer (lane 1) and in TMACl buffer containing 1 M KCl (lane 2). Samples were incubated for 3 h at 37 °C. The lane on the right shows DNA size markers.

in Figure 10C, it is a structural analogue of the double-crossover complex (Figure 10D) used as a construction tile by Seeman and co-workers.[9−11] A key difference between the two tiles is that the [(H·I)T(L·M)]$_2$ tile may be broken down and reconstructed from its synaptic precursor (H·I)T(L·M) (Figure 10A) by controlling solution conditions (i.e., by adding or removing potassium) and without the need for a topological untangling of strands, as might be required for the double-crossover. Figure 10C shows schematically that either two, four, or six unique sticky end sequences can be associated with the [(H·I)T(L·M)]$_2$ tile, in precise orientational relationships to one another. Such a tile, either by itself or in combination with double-crossover tiles (Figure 10D), could be used to generate a variety of repeating structural arrays. An interesting new flexibility in assembling DNA superstructures or repeating arrays using *both* the [(H·I)T(L·M)]$_2$-like and double-crossover modules might be that assembly could be carried out in two different sequential

orders, depending on the superstructure being assembled. For instance, the sticky end annealing processes of the double-crossovers (which are favored by the overall solution ionic strength but not by *specific* Group IA or IIA cations) could either precede or follow the G-G domain-mediated synaptic annealings (which are favored specifically by potassium ions and disfavored by lithium ions).

Conclusion

A key result that we report in this paper is the property of synaptic specificity, observable in solution mixtures of two synapsable duplexes with nonidentical G-G domains. In this paper, we have shown that experimental conditions can be established in which (a) two nonidentical synapsable duplexes *both* dimerize by synapsis, but overwhelmingly to *self* (*simultaneous* specificity), and (b) one duplex at a time dimerizes selectively to give its homo-synapsed dimer; whereas the other duplex remains undimerized (*individual* specificity). Undoubtedly, many more such self-specific G-G domains can be designed, and we are working intensively on this problem. The availability of a number of such domains will facilitate the self-assembly of complex DNA superstructures. In this paper, we have demonstrated a simple example of the utility of the simultaneous specificity scheme, whereby two different G-G mismatch domains incorporated into the arms of a three-way junction DNA molecule, (H·I)T(L·M), were able to synapse, upon the addition of an stabilizing cation (potassium), to form a defined symmetrical dimer, [(H·I)T(L·M)]$_2$. The use and versatility of controlled individual dimerization of G-G domains within a single DNA double helix may be particularly useful in the construction of complex objects.